GeoScienceWorld
Lithosphere
Volume 2022, Article ID 5775275, 14 pages
https://doi.org/10.2113/2022/5775275

Lithosphere

Research Article

The Effect of Roughness on the Nonlinear Flow in a Single Fracture with Sudden Aperture Change

Zhou Chen,[1] **Zhengying Tian**,[1] **Hongbin Zhan**,[2] **Jingtao Huang**,[1] **Yong Huang**,[1] **Yunbo Wei**,[1] **and Xing Ma**[1]

[1]*School of Earth Science and Engineering, Hohai University, Nanjing 210098, China*
[2]*Department of Geology and Geophysics, Texas A&M University, College Station, TX, USA*

Correspondence should be addressed to Zhou Chen; chenzhoucly@hhu.edu.cn and Hongbin Zhan; zhan@geos.tamu.edu

Received 14 April 2022; Accepted 4 June 2022; Published 27 June 2022

Academic Editor: Xiaoding Xu

Abrupt changes in aperture (sudden expansion and contraction) are commonly seen in naturally occurred or artificial single fractures. The relevant research mainly focuses on the changes in fluid properties caused by the sudden expansion of the aperture in smooth parallel fractures. To investigate the effects of roughness on the nonlinear flow properties in a single rough fracture with abruptly aperture change (SF-AC), the flow characteristics of the fractures under different Reynolds numbers R_e (50~2000) are simulated by the turbulence k-ε steady-state modulus with the Naiver-Stokes equation. The results show that, in a rough SF-AC, the growth of the eddy and the flow path deflection of the mainstream zone are more obvious than those in a smooth SF-AC, and the discrepancies between the rough and smooth SF-ACs become even more obvious when the relative roughness and/or R_e values become greater. The increase of the fracture roughness leads to the generation of more local eddies on the rough SF-ACs and enhances the flow path deflection in the sudden expansion fracture. The number of eddies increases with R_e, and the size of eddy area increases linearly with R_e at first. When R_e reaches a value of 300-500, the growth rate of the eddy size slows down and then stabilizes. Groundwater flow in a rough SF-AC follows a clearly visible nonlinear (or non-Darcy) flow law other than the linear Darcy's law. The Forchheimer equation fits the hydraulic gradient-velocity (J-v) better than the linear Darcy's law. The corresponding critical R_e value at which the nonlinear flow starts to dominate in a rough SF-AC is around 300~500.

1. Introduction

Flow in a single fracture (SF) is an important issue in many fields, including structural geology, hydrogeology, environmental, and geotechnical engineering, and petroleum engineering [1–7]. Previous studies have shown that fracture aperture changes (expansion or contraction), fracture surface contact, and fracture roughness have played major roles of affecting fluid flow in a SF [8–10]. The variation of fracture apertures causes fluctuation of streamlines when the Reynolds number (R_e) is relatively small and generates chaotic or turbulent flow when R_e is relatively large [11–14]. When the R_e becomes sufficiently large, velocity contrasts between middle of the fracture and near the fracture walls become so large that dispersive transport becomes increasingly non-Fickian (or abnormal), meaning that the dispersive mass flux is no longer proportional to the concentration gradient [15]. The contact of the fracture surface leads to the development of preferential flow, which aggravates the situation, leading to further non-Fickian transport phenomenon [8, 16]. The presence of fracture roughness further exacerbates the situation, increasing the nonlinearity of water flow and the non-Fickian phenomenon of solute or heat transport [7, 17, 18].

An important question that has not yet been satisfactorily answered is how to relate fluid flow with the geometry and roughness of the fracture, especially when the apertures of the fracture change abruptly [19, 20]. In recent decades, great efforts have been made to study fluid flow through abruptly expanding pipes, plates, or fractures [21–26]. A SF with an abruptly changing aperture (denoted as SF-AC) often has eddies/recirculation areas that result in extended

residence time for water flow and solute transport. The recirculation areas can also become habitats for microbial growth which may enhance the degradation of some organic contaminants. Both experimental and theoretical studies have shown that the size of eddies is mainly determined by the expansion ratio (E), defined as the ratio of larger to smaller apertures (D/d), and the R_e [27–30]. The fluctuation of streamlines and the growth of the characteristic eddy length (l), defined in this study as the length from the left edge to the right edge of the eddy along the flow direction, are two primary issues related to the flow in a SF-AC.

Experimental and numerical studies have shown that the $l - R_e$ relationship in a symmetric and abruptly expanding channel (similar to a smooth surface single fracture) starts to bifurcate at a critical Reynolds number (R_ec) [24, 28, 31]. The value of R_ec is closely related to the geometric parameters of the abruptly expanding channel or fracture. Qian et al. [32] summarized the relationship between R_ec and E and found the R_ec values ranging from 40.45 to 500 (based on the upstream channel height and the average velocity) with an expansion ratio E of 3. Battaglia et al. [33] numerically studied bifurcation of low-R_e flow in symmetric channels and found that the critical values decreased when E increased (e.g., R_ec = 446 at $E = 1.5$ and R_ec = 43 at $E = 5$). With regard to quantification of l, an approximately linear relationship existed between E and l when R_e was less than 210 [33]. However, Milos et al. [34] and Makino et al. [35] found that l increased linearly with R_e until it reached 400 and then decreased with R_e; it became nearly constant when R_e was greater than 1000.

Besides the influence of E and R_e on flow and transport in a single fracture, many studies have been presented to describe experimentally and numerically the effect of roughness on flow through a single rough fracture as well [14, 36–38]. When surface fluctuations (or deviations from a flat or smooth surface) are large compared to the average aperture, the flow was forced to move along sinuous pathways (when flow was still in the laminar flow regime) that create additional viscous friction [36, 39]. At low R_e, when the inertial effect on flow can be neglected, the relationship between the flow rate through the fracture and the pressure gradient driving the flow is linear or Darcy. The local cubic law (LCL), based on Darcy's law, was established by Lomize [40] to describe fluid flow through a SF idealized as a series of parallel plates.

$$Q = -\frac{\rho g b^3}{12\mu}\frac{dh}{dx}, \qquad v = -\frac{\rho g b^2}{12\mu}J, \tag{1}$$

where Q is the volumetric discharge rate (m^3/s), ρ is water density ($kg/m^{3)}$, g is the gravitational acceleration (m/s^2), b is the fracture aperture, μ is kinematic viscosity (Pa·s), h is water head (m), v is flow velocity (m/s) and it equals the Darcy velocity or specific discharge because the fracture is open with a porosity of unity, and $J = dh/dx$ is hydraulic gradient (dimensionless) along the average flow direction which is the x axis.

The LCL is valid when the flow is linear and the R_e value is sufficiently small, but it is usually not suitable for describing the flow in a rough and unparalleled fracture at laboratory and field scales even when the R_e value is relatively small [37, 38, 41–45]. Forchheimer [46] proposed an empirical quadratic relationship to describe the pressure gradient as a function of flow rate in porous media when the inertial effect became nonnegligible [36, 47]. This relationship (namely the Forchheimer equation) has been used in numerous studies to describe flow in SF and is usually written as follows:

$$J = -\left(Av + Bv^2\right) = -\left(\frac{\mu}{K\rho g}v + \frac{\beta}{g}v^2\right), \tag{2}$$

where A (s/m) and B (s^2/m^2) are the linear and inertial coefficients, respectively; K is the hydraulic conductivity (m/s); and β (m^{-1}) is the Forchheimer coefficient, which, in principle, depends only on the geometry of the fracture and not on the flow conditions or fluid properties [38]. The Forchheimer number (F_o) is defined as the ratio between the quadratic and linear terms, which can be interpreted as the ratio of the nonlinear inertial contributions to the pressure drop to the linear term that accounts for viscous resistance [48–53].

$$F_o = \frac{Bv^2}{Av} = \frac{Bv}{A}. \tag{3}$$

The F_o indicates the magnitude of relative deviation from the linear regime and it is possible to use it to define the onset of nonlinear flow [50]. In addition, Zeng and Grigg [52] suggested that a nonlinear coefficient α could be defined as follows:

$$\alpha = \frac{Bv^2}{Av + Bv^2} = \frac{F_o}{1 + F_o}. \tag{4}$$

Another dimensionless parameter for analyzing inertial forces versus viscous forces is R_e, which is defined as follows for flow in a SF:

$$R_e = \frac{2\nu b}{\nu}, \tag{5}$$

where ν is the dynamic viscosity of water (m^2/s), equal to 1.007×10^{-6} m^2/s at temperature 20°C.

Previous researches concerning flow and transport in a SF have mainly focused on the changes in fluid properties caused by the sudden expansion of the aperture in smooth, parallel fractures. The purpose of this investigation is to study the effects of roughness on the nonlinear flow properties in a single rough fracture with abrupt aperture, and proper SF models containing the sudden expansion and contraction of the aperture were first formed. Then, we can simulate the flow characteristics under different R_e (50~2000) by

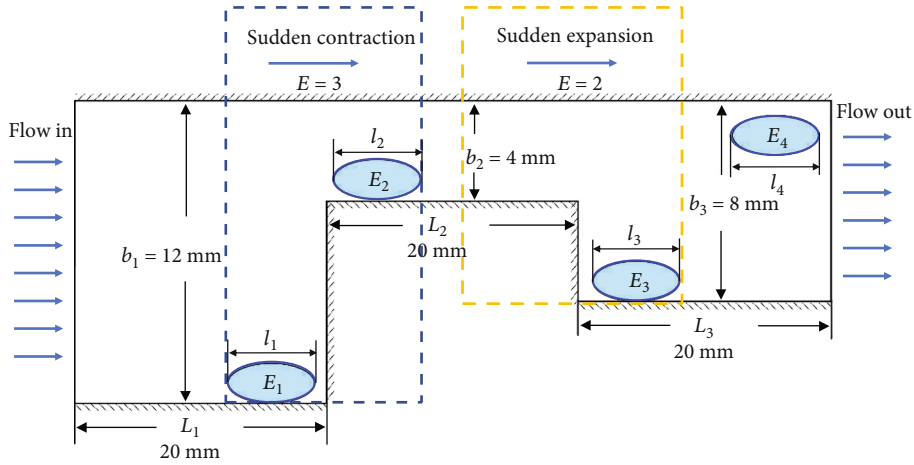

FIGURE 1: Diagram of a smooth single fracture with abrupt aperture change. The model consists of three sections connected in series with apertures of 12 mm, 4 mm, and 8 mm, respectively, divided into two parts: a sudden contraction part ($L_1 \longrightarrow L_2$), and a sudden expansion part ($L_2 \longrightarrow L_3$). Eddies (E_1, E_2, E_3, and E_4) may be formed in four places, and l_1, l_2, l_3, and l_4 represent the lengths of the eddies, respectively.

coupling the turbulence k-ε (k is the kinetic energy of the turbulent pulsation; the larger the k, the larger the length and time scale of the turbulent pulsation; ε is the dissipation rate of the turbulent pulsation momentum; the larger the ε is, the smaller the length and time scale of the turbulent pulsation are) steady-state modulus with the Naiver-Stokes equation. The changes in streamline formations and laminar flow regimes, the changes in the number and length of eddies, and the $l - R_e$ relationship were studied and compared with those with smooth surfaces in a SF.

2. Conceptual Model and Simulations

Since the focus of this study is on the effect of aperture change (sudden expansion and contraction) and roughness on the flow through a single fracture, an asymmetric smooth SF-AC (see Figure 1) and rough SF-AC are constructed. The model consists of three sections connected in series with apertures of 12 mm (the 1st section), 4 mm (the 2nd section), and 8 mm (the 3rd section), respectively, divided into two parts: a sudden contraction part ($L_1 \longrightarrow L_2$) when the aperture changes from 12 mm to 4 mm, and a sudden expansion part ($L_2 \longrightarrow L_3$) when the aperture changes from 4 mm to 8 mm. The lengths of sections with apertures of 12 mm, 4 mm, and 8 mm are identical (20 mm). According to our numerical exercises, eddies may be formed in four places in Figure 1, the first eddy (E_1) is near the lower corner when the aperture changes from 12 mm to 4 mm, the second eddy (E_2) is at the lower beginning portion of the narrowest fracture section (with a 4 mm aperture), the third eddy (E_3) is near the lower corner after the fracture aperture is expanded from 4 mm to 8 mm, and the fourth eddy (E_4) is at the upper corner of the fracture section (with a 8 mm aperture) near the exit plane. l_1, l_2, l_3, and l_4 represent the lengths of the first, second, third, and fourth eddies, respectively. The SF is expected to extend to infinity along the direction perpendicular to the cross-sectional area shown in Figure 1; thus, the simulation will be conducted in a cross-sectional plane (or the xz plane) where the positive x axis is pointing to the right horizontally, and the z axis is upward vertical. The origin of the Cartesian coordinate system is at the intersection of the left (vertical) boundary and section L_1. The fracture opening is so small that the gravity effect is irrelevant during the entire simulation. The fluid is assumed to be incompressible and Newtonian and isothermal as well. The fracture walls are impermeable to flow. A point to note is that the eddies may not be formed at the same time, and depending on the flow conditions, some eddies may not be formed at all during the entire simulation time.

The rough SF-ACs were constructed by replacing the smooth upper and lower walls of the fractures in Figure 1 with rough fracture walls. Many studies [54, 55] reported that the geometry of natural fracture walls generally has self-affine properties and the exponent H is a measure of fracture roughness, defined as the Hurst exponent with a range from 0 to 1. In this study, we used the successive random addition technique [56–58] to generate the self-affine fracture wall with an H value of 0.5. The roughness height (or fracture asperity) (Δ) of the generated self-affine fracture wall ranging from -0.0008 to 0.62 mm with an average roughness height of 0.024 mm and a standard deviation of 0.155 mm, where the value of Δ is measured against a uniform horizontal base. The rough SF-ACs were constructed by replacing each fracture walls (20 mm long) in Figure 1 with a generated self-affine fracture wall with $H = 0.5$ (Figure 2).

The original roughness height of the generated self-affine fracture wall in Figure 2 is denoted as a reference roughness height Δ_0, and this reference roughness height is subsequently increased by factors of 2.5, 3, 3.5, and 4 to obtain four more groups of rough fractures. The relative roughness (ω) is defined as the ratio between the average roughness height and the apertures of the corresponding (smooth) sections of the fracture (before the addition of fracture

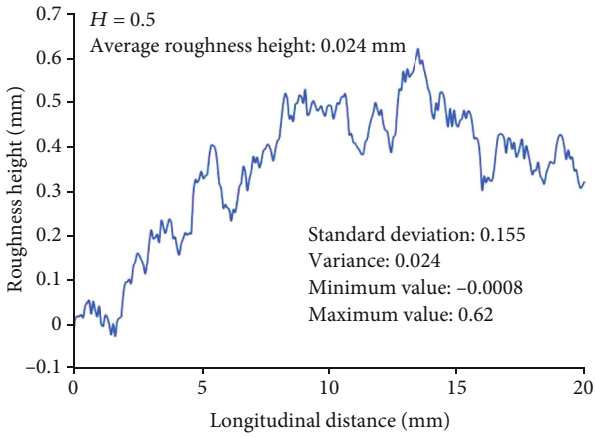

Figure 2: The generated self-affine fracture wall with $H = 0.5$. The roughness height (Δ) of the generated self-affine fracture wall ranging from -0.0008 to 0.62 mm with an average roughness height of 0.024 mm and a standard deviation of 0.155 mm, where the value of Δ is measured against a uniform horizontal base.

Table 1: Characteristic parameters of roughness and aperture in SF-ACs.

Roughness height	Average Δ (mm)	ω $b = 4$ mm	$b = 8$ mm	$b = 12$ mm	Average ω
Δ_0	0.34	8.5%	4.3%	0.7%	4.5%
$2.5\Delta_0$	0.85	21.3%	10.6%	1.8%	11.2%
$3\Delta_0$	1.02	25.5%	12.8%	2.1%	13.5%
$3.5\Delta_0$	1.19	29.8%	14.9%	2.5%	15.7%
$4\Delta_0$	1.36	34.0%	17.0%	2.8%	17.9%

roughness). A total of five groups of SF-ACs were generated and the characteristic parameters can be seen in Table 1.

The Navier-Stokes equation is used to describe incompressible fluid flow in both smooth and rough factures and is as follows:

$$\frac{\partial u}{\partial t} + u \cdot \nabla u = -\frac{\nabla P}{\rho} + \nu \nabla^2 u, \tag{6}$$

where P is fluid pressure (Pa), t is time (s), u is the fluid velocity vector (dimensionless), and ∇^2 is the Laplacian operator.

In this study, the standard $k - \varepsilon$ model in COMSOL Multiphysics is used to calculate the flow field. The $k - \varepsilon$ model is a two-equation model consisting of the turbulent kinetic energy k and the turbulent dissipation rate ε [59]. The flow model is solved based on the finite-element method implemented in COMSOL Multiphysics. In this study, we have used standard water properties at 20°C (e.g., $\rho = 998.2$ kg/m^3 and $\mu = 1.010 \times 10^{-3}$ Pa·s). The fracture walls were considered nonslip boundaries. A constant discharge rate is set at the entrance of the fracture, and the outlet pressure is set to zero by default. Quadrilateral dense meshing is performed near the rough fracture wall, and regular free triangular meshing is performed for the rest region of the model to accurately describe the flow at the fracture wall and in the region of sudden aperture change without substantially increasing the computational expense. Flow conditions with a R_e of 50~2000 and a relative roughness (ω) of 4.5% ~ 17.9% are simulated. There are approximately 56,433 triangular elements, 9697 quadrilateral elements, and 39,377 nodes in the discretized fracture domain ($\omega = 13.5\%$). Mesh independence analysis is performed to ensure the numerical stability and accuracy. The grid of model is illustrated in Figure 3 (for an example of the grid at $\omega = 4.5\%$ and 17.9%).

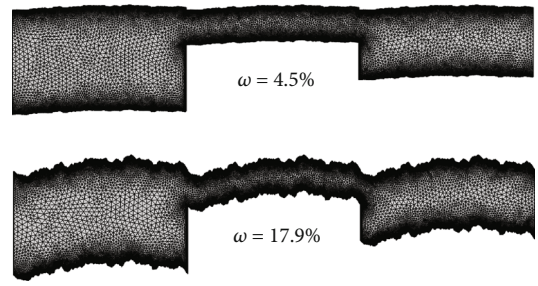

Figure 3: Grid of the rough fracture model. Quadrilateral dense meshing is performed near the rough fracture wall and regular free triangular meshing is performed for the rest region of the model to accurately describe the flow at the fracture wall and in the region of sudden aperture change without substantially increasing the computational expense.

3. Results and Discussion

3.1. Flow Characteristics in Smooth SF-AC. First, we examine the flow characteristics in smooth SF-AC. As can be seen from the streamline diagram (Figure 4), the streamline is laminar and the flow velocity almost does not change in most parts of section L_1. When approaching the sudden contraction regime from L_1 to L_2, the flow velocity increases rapidly and reaches the maximum flow velocity shortly after reaching the L_2 section. In most of the L_2 section, the streamlines are still laminar and the eddy forms in the lower left corner of the L_2 section (the l_2 area) when R_e is greater than 350, as shown in Figure 4(b). The fluid reaches the L_3 section after experiencing the sudden expansion. In this fracture section, the fluid has two distinctive characteristics in the main flow region (with relatively high velocity) and the quasistagnant region (with relatively low velocity). Flow lines in the main flow region are mostly laminar. Flow lines in the quasistagnant region are also laminar but with an eddy formed in area l_3 in Figure 4. With the increase of R_e, the size of the eddy starts to increase as well. This is similar to the experimental results of symmetric aperture expansion in SF-AC, as investigated by Qian et al. [20]. In the smooth SF-AC, the eddy E_2 and E_3 appear and the eddy E_2 is smaller than that of E_3. Furthermore, l_2 changes only mildly after R_e

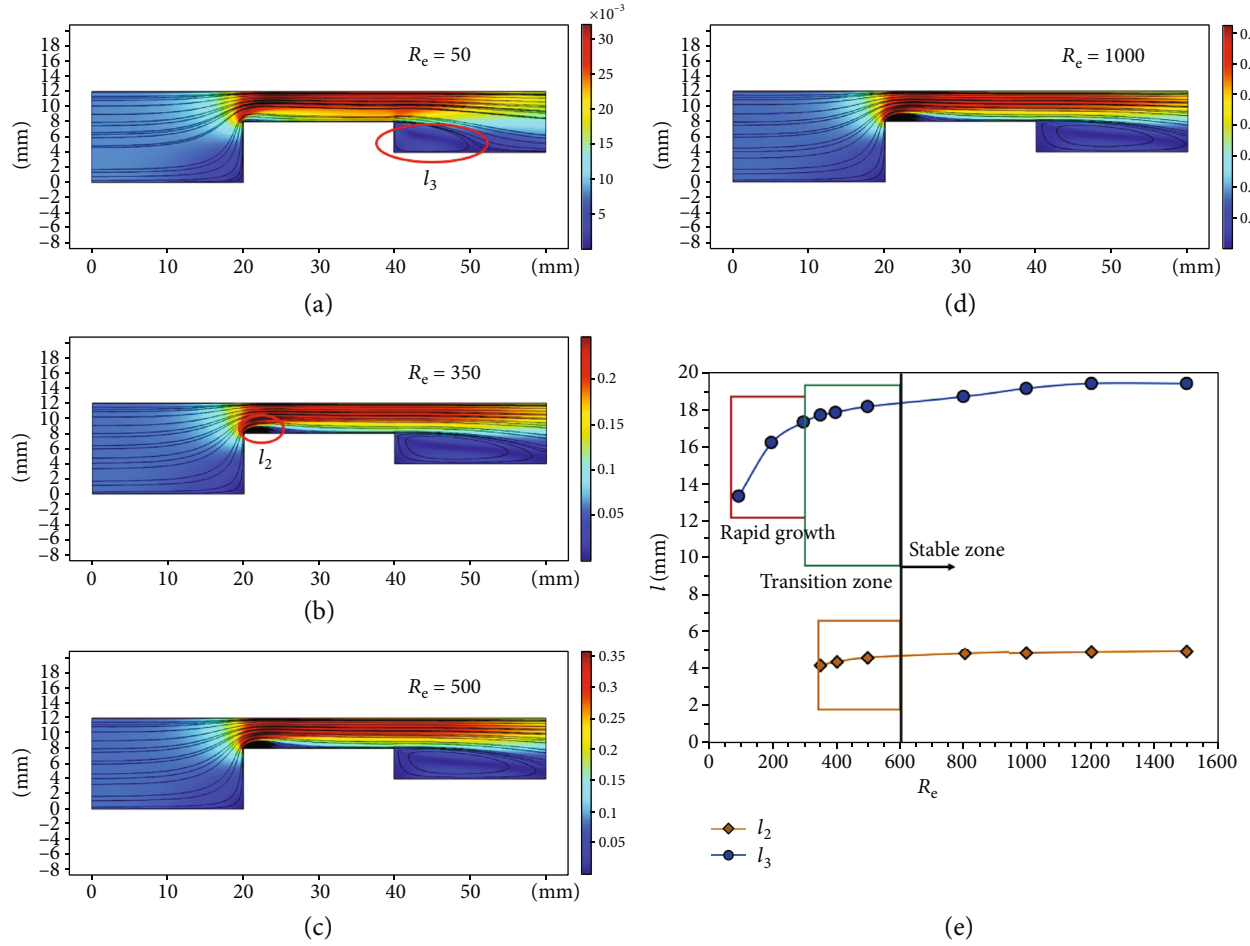

FIGURE 4: Streamline diagram and $l - R_e$ relationship in smooth SF-AC. The fluid has two distinctive characteristics in the main flow region and the quasi-stagnant region. Flow lines in the main flow region are mostly laminar. The eddy appears in both area l_2 and area l_3.

becomes greater than 350. Conversely, the l_3 increases rapidly first when R_e becomes greater than 50, from 13 mm to about 18 mm. However, when R_e becomes greater than 600, the rate of increase for the l_3 slows down substantially and tends to be insensitive to further increase of R_e.

3.2. Flow Characteristics and Impact Factors in Rough SF-AC. The flow characteristics in the rough SF-AC are simulated, and the result can be seen in Figure 5.

We have shown the flow characteristics in the rough SF-AC under different R_e (100~2000) with $\omega = 17.9\%$ in Figures 5(a)–5(d), and different relative roughness (4.5% ~ 17.9%) with R_e at 1000 in Figures 5(c), 5(e)–5(h). The major difference of flow characteristics of the rough SF-AC from that of the smooth SF-AC is that the distinction of the main flow region and the quasi-stagnant region becomes more obvious in the rough SF-AC, and the flow streamlines becomes more tortuous. Furthermore, all four eddies ($E_1 \sim E_4$) emerge for the rough SF-AC, while the observed number of eddies for the smooth SF-AC is less than 4. To investigate the changes of each eddy, we calculated the l-R_e relationship under different R_e and ω for the rough SF-AC case (see Figure 6). The corresponding value of R_e of the transitional zone for the five different rough SF-ACs is approximately in the range from 300 to 500. A larger relative roughness (ω) leads to a more obvious flowpath deflection trend and a smaller size of eddy l_3.

3.2.1. The Influence of R_e and Relative Roughness on Flow Characteristics. From Figures 5(a)–5(d), it can be seen that at $\omega = 17.9\%$, when R_e gradually increases, the degree of streamline variation (or tortuosity) increases and the streamlines in the main flow region of the L_3 section exhibits a downward attachment trend (or flowpath deflection trend). This deflection trend can be explained by the Coandă effect [60], the basic idea of the Coandă effect is that jet fluids tend to be attracted to nearby solid surfaces. Comparing the flowpath deflection effect at different roughness, we find that a larger relative roughness leads to a more pronounced flowpath deflection effect. The reason could be that as the roughness of the fracture increases, the friction of the fluid on the rough fracture wall increases and the energy loss due to friction increases accordingly. As a result, the area of the high velocity main flow region gradually decreases and correspondingly the area of the low velocity quasistagnant region gradually increases.

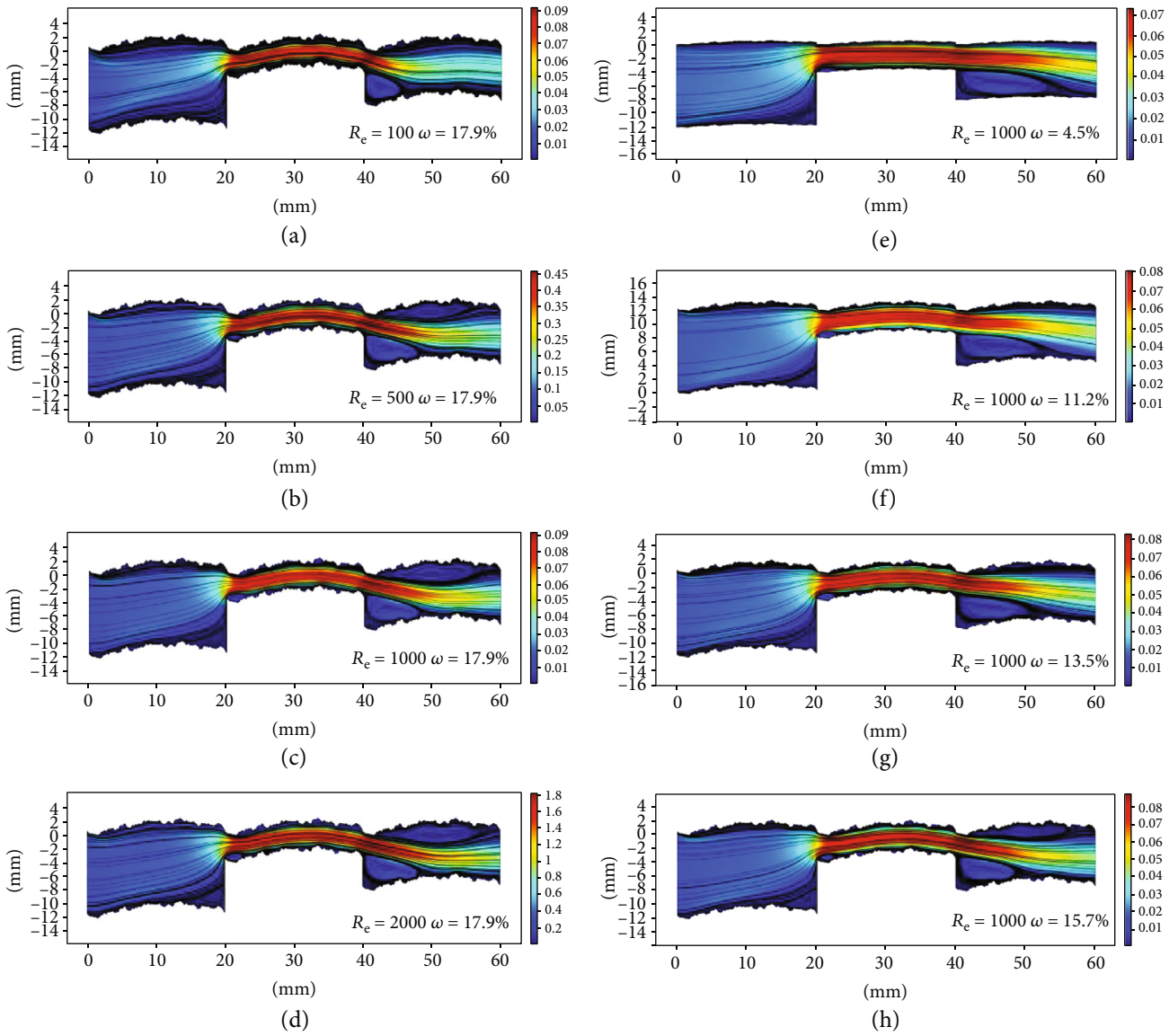

Figure 5: Streamline diagram under different R_e (left) and ω (right) in rough SF-AC. The flowpath deflection of the main flow region occurs. And a larger value of R_e results in a larger region of flowpath deflection.

From Figures 5 and 6, it can be seen that when R_e is less than 200, eddies are generated in the areas E_2 and E_3 in the sections of L_2 and L_3. When R_e is greater than 200, several eddies of different sizes are generated in the rough wall SF-AC, of which the two eddies E_1 and E_4 are the most obvious. When R_e is in the range of 100~300, the eddy size increases rapidly, and when R_e reaches the transitional range of 300~500, the growth rate of the eddy size slows down and stabilizes. This is consistent with the simulation result of the study for a smooth SF-AC and the result of Makino et al. [35].

For a relatively small value of R_e (less than 300), the size of eddy increases linearly and rapidly as R_e increases. However, as R_e further increases, the rate of change of the eddy size slows down and then becomes stable. Here, the region between the linear growth zone and the stable zone is called the transitional zone. From Figure 6, it can be seen that the corresponding value of R_e for the transitional zone for the five different rough SF-ACs is approximately in the range of 300 to 500.

From Figures 6(a)–6(e), we can see that there is always an eddy (l_3) in the rough SF-ACs. To study the effect of the relative roughness on the eddy size, the relationship between the l_3 and R_e in five different rough SF-ACs is compared and the result is shown in Figure 6(f). When ω = 4.5%, the l_3 ranges from 7 mm to 19 mm, while when ω increases to 17.9%, the l_3 decreases to 5 mm to 8 mm. This is because the abovementioned phenomenon of flowpath deflection trend of the main flow region occurs in the region of sudden expansion. A larger relative roughness (ω) leads to a more obvious flowpath deflection trend and a smaller size of l_3. Accordingly, the l_4 in the upper left corner of section L_3 gradually increases.

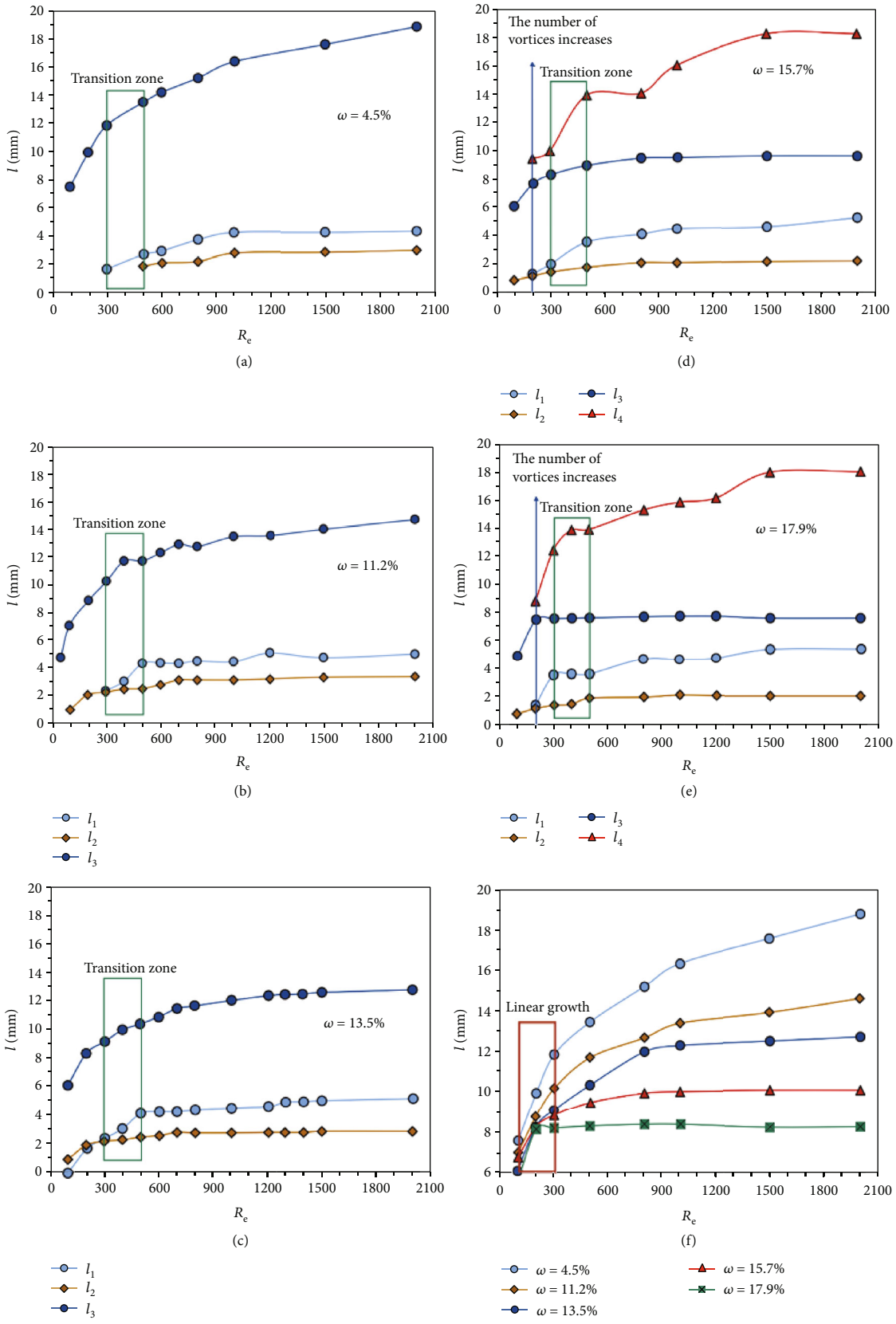

FIGURE 6: l-R_e relationship under different R_e and ω in rough SF-AC. The corresponding value of R_e for the transitional zone for the five different rough SF-ACs is approximately in the range of 300 to 500. A larger relative roughness (ω) leads to a more obvious flowpath deflection trend and a smaller size of eddy l_3.

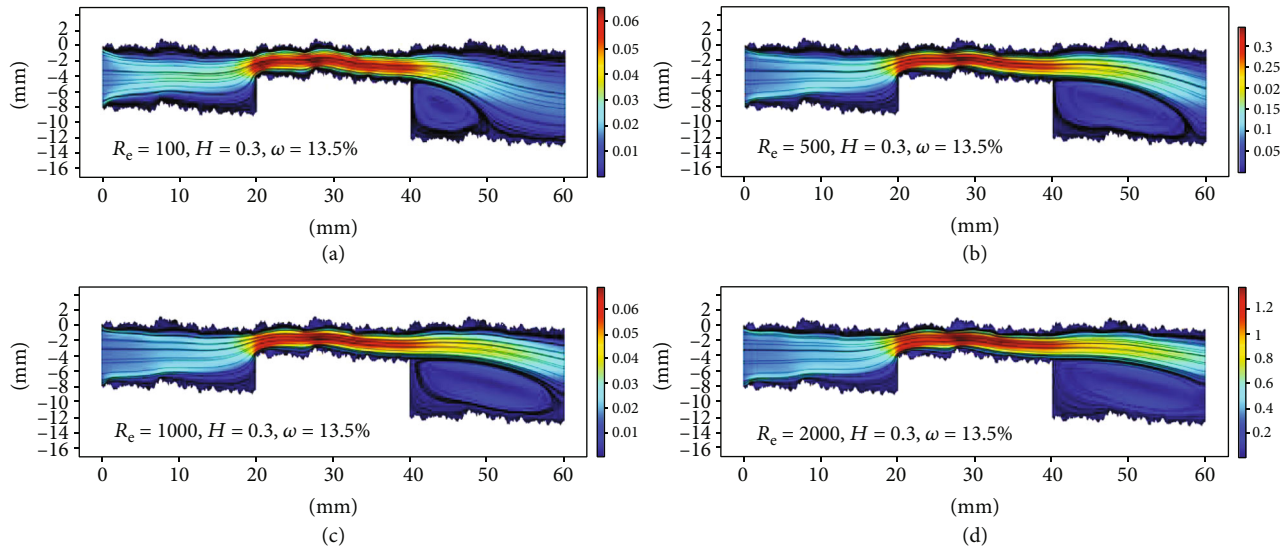

Figure 7: Velocity streamline diagram and l-R_e relationship in rough SF-AC ($H = 0.3$, $\omega = 13.5\%$). The increase in roughness heterogeneity in the sudden constriction section increases the number of small eddies near the fracture walls.

3.2.2. Flow Characteristics in Rough SF-AC under Different H. To study the flow characteristics in rough SF-AC with different degrees of roughness (as reflected by the Hurst exponent H), flow through a SF-AC with $H = 0.3$ at $\omega = 13.5\%$ is simulated, and the result is shown in Figures 7 and 8 as an example of demonstration. From Dou et al. [8], we know that a smaller H value means a greater degree of roughness. The diagram of streamlines is shown in Figure 7. From this figure, it can be seen that the streamlines and the main flow region in the SF-AC for $H = 0.3$ behave similarly as that of $H = 0.5$. The flowpath deflection of the main flow region occurs when the flow passes through the expansion section. And a larger value of R_e results in a larger region of flowpath deflection. The number of eddies and the corresponding positions are also the same as for $H = 0.5$ and $\omega = 13.5\%$.

Comparing the l-R_e relationship at $H = 0.5$ (Figure 6(c)) and $H = 0.3$ (Figure 7), the trend of eddy development is approximately the same for these two cases. The eddies E_1 and E_2 are smaller in the sudden constriction section at $H = 0.3$, and the eddy E_3 of $H = 0.3$ is larger than that of $H = 0.5$, and the eddy E_3 is always present in the rough SF-AC at $H = 0.3$. When R_e are greater than 200, eddies E_1 and E_2 are formed, but the eddy size is smaller and does not change significantly compared to $H = 0.3$. At $R_e \geq 800$, the growth rate of l_3 slows down and expands to the entire section L_3 due to the limited length of the fracture.

From Figures 7(a)–7(d) and 8, it can be seen that the increase in roughness heterogeneity in the sudden constriction section increases the number of small eddies near the fracture walls, resulting in l_1 and l_2 being smaller than those at $H = 0.5$. However, in the sudden expansion section, the increase in roughness enhances the degree of flowpath deflection, resulting in the l_3 and the size of the eddy being larger than their counterparts at $H = 0.5$. The above situation shows that the increase of the roughness of the SF-AC leads to the generation of more local eddies and enhances the flowpath deflection in the sudden expansion section of the fracture.

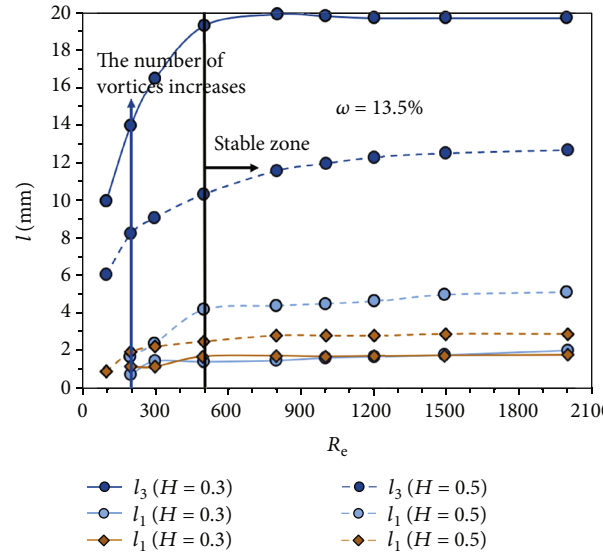

Figure 8: l-R_e relationship in rough SF-AC ($H = 0.3$, $\omega = 13.5\%$). In the sudden expansion section, the increase in roughness enhances the degree of flowpath deflection.

3.3. Growth of the Low-Velocity Area in Smooth and Rough SF-AC. In the previous two sections, we have discussed the occurrence and evolutionary features of the main eddies through the SF-ACs. However, in addition to the main eddies, many relatively small eddies also develop near the rough fracture walls. The existence of these small eddies also affects the water flow and solute transport quite considerably.

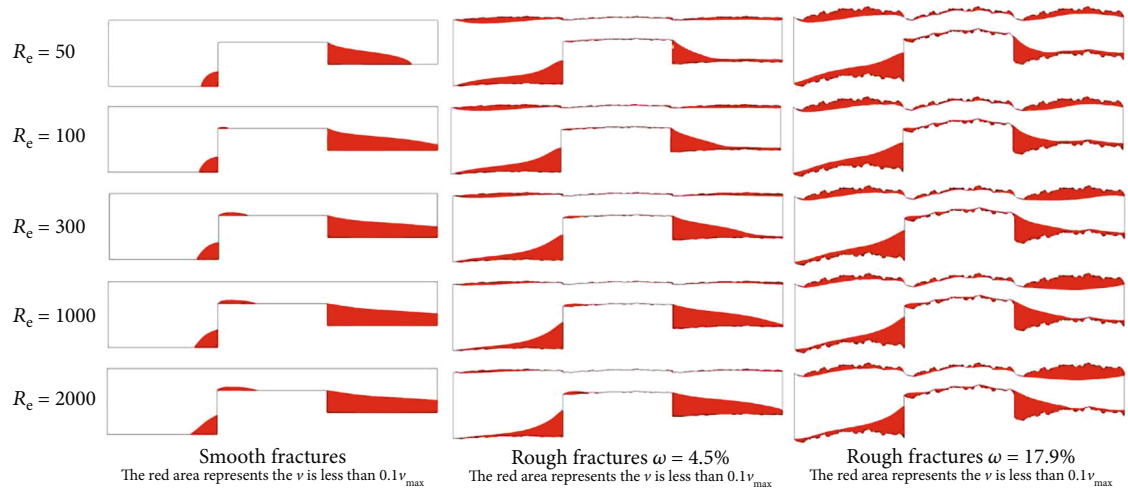

FIGURE 9: Low-velocity area distribution in smooth and rough SF-AC. In smooth SF-ACs, there is no low-velocity area near the upper fracture wall, low-velocity areas appear at L_1, L_2, and L_3 near the lower fracture wall, and the area increases with R_e; in rough SF-ACs, low-velocity areas appeared near both the upper and lower fracture walls, and the area increased with R_e.

To analyze the evolution of the low-velocity area (defined as the area where the maximum flow velocity is equal to 10% of the maximum velocity over the entire fracture), we have plotted the distribution of the low-velocity area distribution of smooth SF-ACs and rough SF-ACs with relative roughness of 4.5% and 17.9% under different R_e (see Figure 9).

In smooth SF-ACs, there is no low-velocity area near the upper fracture wall, low-velocity areas appear at L_1, L_2, and L_3 near the lower fracture wall, and the area increases with R_e; in rough SF-ACs, low-velocity areas appeared near both the upper and lower fracture walls, and the area increased with R_e. In smooth SF-ACs, the low-velocity areas increased slowly at $R_e > 500$; in rough SF-ACs, when $R_e > 300$, the low-velocity areas slowly increased. These observations mean that due to roughness, the low-velocity areas in rough SF-ACs are larger than those in smooth SF-ACs, and the low-velocity areas in rough SF-ACs always present while they may or may not present in smooth SF-ACs. Another notable point is that the changes of those low-velocity areas appear to be less sensitive to the R_e values, regardless of whether the fractures are smooth or rough.

To investigate the effect of relative roughness on low-velocity area, we compared the change of low-velocity area at relative roughness of $\omega = 4.5\% \sim 17.9\%$ at $R_e = 1000$ (see Figure 10 for detail). With the increase of R_e, the proportion of low-velocity area increases from 16.1% to 24.5%, indicating that with the increase of ω, the low-velocity area increases and the protion of increase mostly occurred in section L_4. This is because with the increase in ω, the flowpath deflection of flow becomes more prominent.

3.4. Nonlinear Flow in Rough SF-AC. To analyze the effect of roughness on nonlinear flow (or non-Darcy flow) in SF-ACs, the relationship between the hydraulic gradient (J) and average velocity (v) under different relative roughness was first compared and fitted, where J is the difference in average hydraulic pressures at the inlet and outlet divided by the length of the fracture and v is computed using the v at the outlet of the fracture. The fitted equations use the linear local cube law (LCL) (based on Darcy's law) and the nonlinear (or non-Darcy) Forchheimer equation, respectively. The results can be seen in Figure 11 and Table 2.

From the results, the J-v relationship in the rough SF-AC is clearly nonlinear and the fitting result of the Forchheimer equation is better than that of the linear LCL equation. This shows that in five groups of rough SF-ACs with different ω, the groundwater flow is nonlinear (or non-Darcy) and the degree of nonlinearity increases with ω.

To further investigate the influence of fracture roughness on the flow nonlinearity, the Forchheimer number (F_o) in Equation (3) and the nonlinear coefficient α in Equation (4) were analyzed. Here, F_o is defined as the ratio of nonlinear to linear pressure drop in the Forchheimer equation [49–52]. The results can be seen in Figures 12 and 13.

Zeng and Grigg [52] explained the physical meaning of F_o, which is the ratio between the pressure gradient required to overcome the inertial force and the pressure gradient of the viscous force. Ghane et al. [61] found that the Forchheimer equation adequately described the flow of water through woodchip columns experimentally and determined the F_o value at 0.31 and the corresponding value for α to be 0.24. Laboratory measurements of non-Darcy flow coefficients in natural and artificial unconsolidated porous media were made by Macini et al. [62] and suggested that $\alpha = 0.28$ and $F_o = 0.40$ when nonlinear (or non-Darcy) flow occurs in natural sand media.

From Figure 12, it can be seen that F_o increases linearly with R_e and a larger relative roughness leads to a larger corresponding value of F_o. This shows that a larger R_e number leads to a more evident nonlinear phenomenon of groundwater flow in rough SF-ACs (as expected). When R_e is larger than 300, the value of $F_o > 1$, meaning that the inertia term in groundwater flow begins to dominate. Figure 13 shows that α increases linearly when R_e is between 100 and 300.

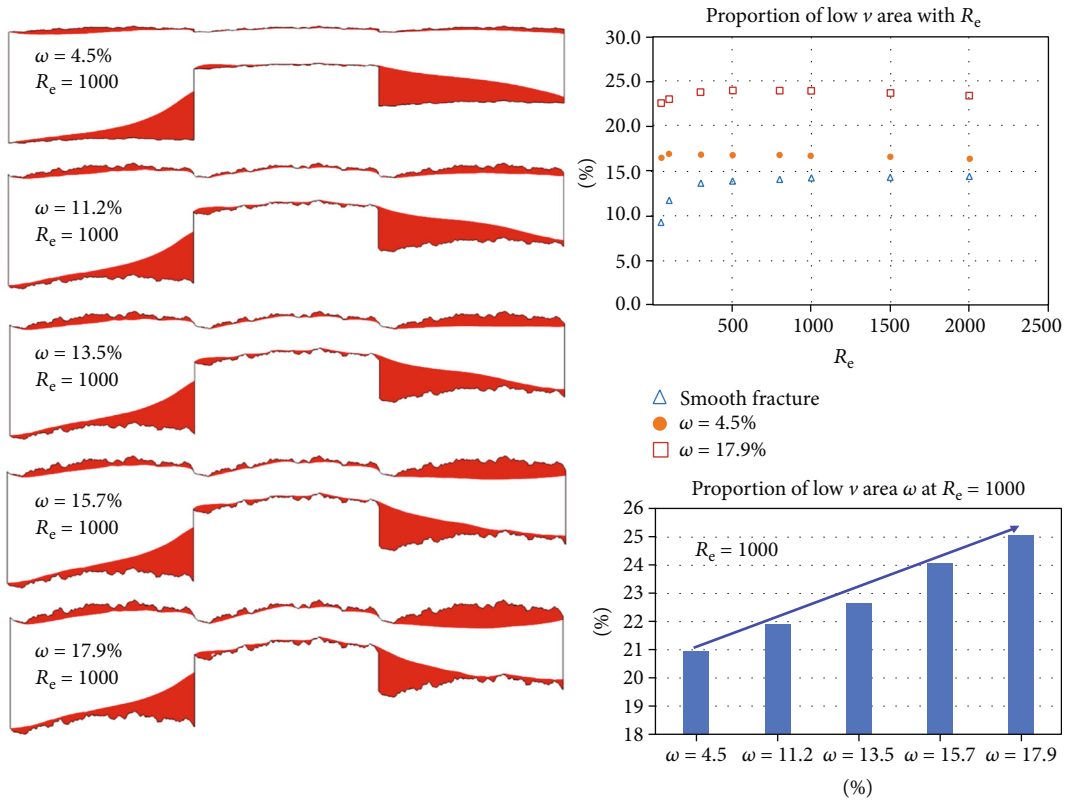

Figure 10: Proportion of low-velocity area under different R_e and ω. Due to roughness, the low-velocity areas in rough SF-ACs are larger than those in smooth SF-ACs, and the low-velocity areas in rough SF-ACs always present while they may or may not present in smooth SF-ACs. With the increase of ω, the low-velocity area increases and the portion of increase mostly occurred in section L_4.

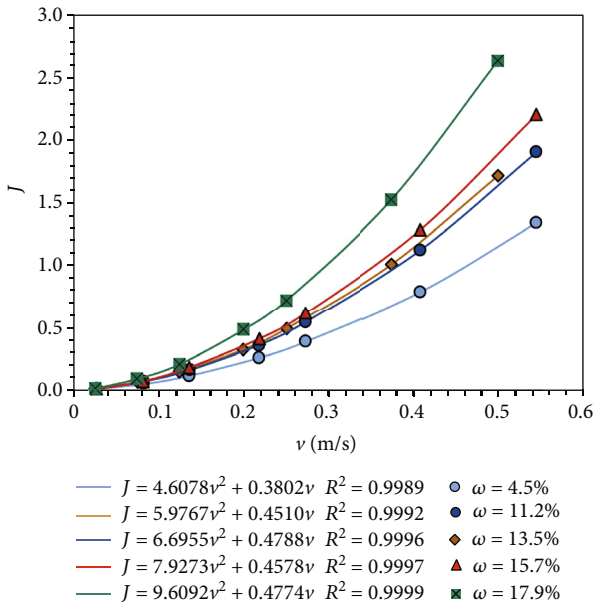

Figure 11: Fitting curves of J-v and by Forchheimer equation in rough SF-AC. The J-v relationship in the rough SF-AC is clearly nonlinear, and the fitting result of the Forchheimer equation is better than that of the linear LCL equation.

Table 2: Fitted results of J-v in rough SF-ACs under different ω.

ω	Forchheimer equation	R^2	LCL	R^2
$\omega = 4.5\%$	$J = 4.6078v^2 + 0.3802v$	0.9989	$J = 2.0026v$	0.9412
$\omega = 11.2\%$	$J = 5.9767v^2 + 0.4510v$	0.9992	$J = 2.8111v$	0.9427
$\omega = 13.5\%$	$J = 6.6955v^2 + 0.4788v$	0.9996	$J = 2.8403v$	0.9391
$\omega = 15.7\%$	$J = 7.9273v^2 + 0.4578v$	0.9997	$J = 3.3042v$	0.9353
$\omega = 17.9\%$	$J = 9.6092v^2 + 0.4774v$	0.9999	$J = 4.2388v$	0.9352

When R_e increases beyond 500, the growth rate of α changes gradually and tends to be stable. Zhou et al. [53] argued that α represented the degree of dominance of the nonlinear term; thus, a larger α meant a higher degree of dominance of the nonlinear term. When the value of α is greater than 0.5, the nonlinear flow is dominant, and vice versa. According to the results of this work, when $\alpha = 0.5$, the corresponding R_e value is about 300, meaning that the groundwater flow in the SF-ACs becomes nonlinear. This observation is consistent with the determined critical R_e value of 300-500 obtained in previous studies.

It can be seen that the groundwater flow in the rough SF-ACs has a relatively obvious nonlinear flow pattern for the simulated condition. From the analysis of the l-R_e relationship, the J-v relationship, and the nonlinear parameters F_o

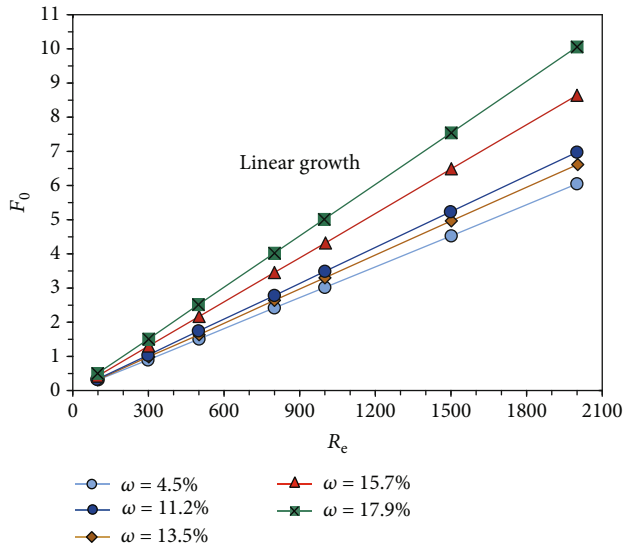

FIGURE 12: Relationship of $F_o - R_e$ in rough SF-AC. F_o increases linearly with R_e and a larger relative roughness leads to a larger corresponding value of F_o. A larger R_e number leads to a more evident nonlinear phenomenon of groundwater flow in rough SF-ACs.

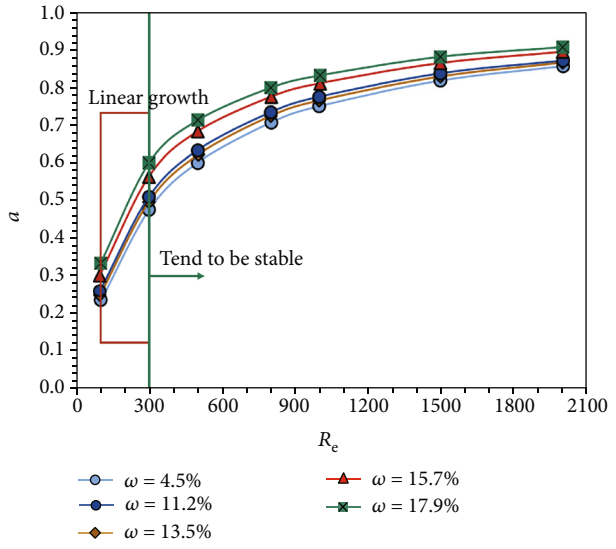

FIGURE 13: Relationship of $\alpha - R_e$ in rough SF-AC. α increases linearly when R_e is between 100 and 300. When R_e increases beyond 500, the growth rate of α changes gradually and tends to be stable. This observation is consistent with the determined critical R_e value of 300-500 obtained in previous studies.

and α, it can be seen that the corresponding critical Reynolds number at which the nonlinear flow begins to dominate is $R_e = 300 \sim 500$.

4. Conclusions

To study the effects of roughness on the nonlinear (or non-Darcy) flow properties in a single rough fracture with abruptly changing apertures, five single fracture models (with each single fracture containing the sudden expansion and contraction of the aperture) were first formed. Then, the flow characteristics of the fractures under different R_e (50~2000) were simulated by the turbulence k-ε steady-state modulus with the Naiver-Stokes equation. The changes in streamline morphology, the changes in the number and length of eddies, and the nonlinear properties of flow through fractures were studied and compared with those in the smooth SF-ACs. The following conclusions can be obtained:

(1) Compared with the flow in smooth SF-ACs, in a rough SF-AC, the growth of the eddy and the flow path deflection of the mainstream zone are more obvious, and the phenomenon is more obvious when the relative roughness and/or R_e are greater; the increase of the roughness leads to the generation of more local eddies near the fracture walls of the rough SF-ACs and enhances the degree of flow path deflection in the sudden expansion section of the fracture

(2) The number of eddies increases with R_e and the size of eddy area increases linearly with R_e at first. When R_e reaches a value of 300-500, the growth rate of the size of eddy slows down and then stabilizes

(3) It can be seen that the groundwater flow in the rough SF-ACs is clearly nonlinear or non-Darcy for the scenarios simulated in this study. The fitting results of hydraulic gradient-specific discharge (or J-v) relationship by the Forchheimer equation is better than that of the linear LCL equation which is based on Darcy's law. The corresponding critical Reynolds number at which the nonlinear flow begins to dominate in rough SF-ACs is around 300~ 500

Data Availability

The data used to support the findings of this study are available from the corresponding author upon request.

Additional Points

Highlights. (1) The growth of the eddy and the deflection of flow paths in the mainstream zone are more evident in the rough SF-AC. (2) The increase of fracture roughness generates more local eddies on the rough SF-ACs and enhances the deflection of flow paths in the sudden expansion fracture. (3) Groundwater flow in a rough SF-AC follows a clearly visible nonlinear flow law and Forchheimer equation fits $J - v$ better than linear Darcy's law. (4) The corresponding critical R_e value at which the nonlinear flow in a rough SF-AC starts to dominate is about 300~ 500

Conflicts of Interest

The authors declare that they have no known competing financial interests or personal relationships that could have appeared to influence the work reported in this paper.

Authors' Contributions

Zhou Chen contributed to the conceptualization and methodology, acquired software, and did the validation, formal analysis, writing-original draft, writing—review and editing, and visualization. Zhengying Tian acquired software and did the formal analysis, and writing—original draft. Hongbin Zhan did the formal analysis, writing—review and editing, and validation. Jingtao Huang did the formal analysis, writing—review and editing, and validation. Yong Huang did the conceptualization and validation. Yunbo Wei acquired resources. Xing Ma acquired software.

Acknowledgments

This work was supported by the Fundamental Research Funds for the Central Universities (Grant number B220202053); the National Key Research and Development Program of China (Grant number 2019YFC1804302); the Key Science and Technology Special Program of Yunnan Province, "Study on key technologies for safe construction and efficient operation of super large water diversion projects under complex geological conditions in Southwest China" (Grant number 202002AF080003); and the key projects of National Natural Science Foundation of China (41831289).

References

[1] Y. Chen, Z. Zhou, J. Wang, Y. Zhao, and Z. Dou, "Quantification and division of unfrozen water content during the freezing process and the influence of soil properties by low-field nuclear magnetic resonance," *Journal of Hydrology*, vol. 602, article 126719, 2021.

[2] Z. Dou, S. X. Tang, X. Y. Zhang et al., "Influence of shear displacement on fluid flow and solute transport in a 3D rough fracture," *Lithosphere*, vol. 2021, no. Special 4, 2021.

[3] X. Y. Liang, Y. K. Zhang, J. Liu, E. Z. Ma, and C. M. Zheng, "Solute transport with linear reactions in porous media with layered structure: a semianalytical model," *Water Resources Research*, vol. 55, no. 6, pp. 5102–5118, 2019.

[4] T. Phillips, T. Bultreys, K. Bisdom et al., "A systematic investigation into the control of roughness on the flow properties of 3D-printed fractures," *Water Resources Research*, vol. 57, no. 4, 2021.

[5] Y. Q. Su, F. Q. Gong, S. Luo, and Z. X. Liu, "Experimental study on energy storage and dissipation characteristics of granite under two-dimensional compression with constant confining pressure," *Journal of Central South University*, vol. 28, no. 3, pp. 848–865, 2021.

[6] J. B. Taylor, A. L. Carrano, and S. G. Kandlikar, "Characterization of the effect of surface roughness and texture on fluid flow –past, present, and future☆," *International Journal of Thermal Sciences*, vol. 45, no. 10, pp. 962–968, 2006.

[7] M. E. Thompson and S. R. Brown, "The effect of anisotropic surface-roughness on flow and transport in fractures," *Journal of Geophysical Research-Solid Earth*, vol. 96, no. B13, pp. 21923–21932, 1991.

[8] Z. Dou, Z. Zhou, J. Wang, and Y. Huang, "Roughness scale dependence of the relationship between tracer longitudinal dispersion and Peclet number in variable-aperture fractures," *Hydrological Processes*, vol. 32, no. 10, pp. 1461–1475, 2018.

[9] S. G. Kandlikar, "Exploring roughness effect on laminar internal flow-are we ready for change?," *Nanoscale and Microscale Thermophysical Engineering*, vol. 12, no. 1, pp. 61–82, 2008.

[10] K. Xing, J. Qian, H. Ma, Q. Luo, and L. Ma, "Characterizing the relationship between non-Darcy effect and hydraulic aperture in rough single fractures," *Water Resources Research*, vol. 57, no. 9, 2021.

[11] D. F. Boutt, G. Grasselli, J. T. Fredrich, B. K. Cook, and J. R. Williams, "Trapping zones: the effect of fracture roughness on the directional anisotropy of fluid flow and colloid transport in a single fracture," *Geophysical Research Letters*, vol. 33, no. 21, 2006.

[12] S. G. Kandlikar, D. Schmitt, A. L. Carrano, and J. B. Taylor, "Characterization of surface roughness effects on pressure drop in single-phase flow in minichannels," *Physics of Fluids*, vol. 17, no. 10, p. 100606, 2005.

[13] L. Wang, M. B. Cardenas, D. T. Slottke, R. A. Ketcham, and J. M. Sharp, "Modification of the local cubic law of fracture flow for weak inertia, tortuosity, and roughness," *Water Resources Research*, vol. 51, no. 4, pp. 2064–2080, 2015.

[14] L. Zou, L. Jing, and V. Cvetkovic, "Roughness decomposition and nonlinear fluid flow in a single rock fracture," *International Journal of Rock Mechanics and Mining Sciences*, vol. 75, pp. 102–118, 2015.

[15] L. Wang and M. B. Cardenas, "Transition from non-Fickian to Fickian longitudinal transport through 3-D rough fractures: scale-(in)sensitivity and roughness dependence," *Journal of Contaminant Hydrology*, vol. 198, pp. 1–10, 2017.

[16] Z. Chen, H. Zhan, G. Zhao, Y. Huang, and Y. Tan, "Effect of roughness on conservative solute transport through synthetic rough single fractures," *Water*, vol. 9, no. 9, p. 656, 2017.

[17] Z. Dou, B. Sleep, H. Zhan, Z. Zhou, and J. Wang, "Multiscale roughness influence on conservative solute transport in self-affine fractures," *International Journal of Heat and Mass Transfer*, vol. 133, pp. 606–618, 2019.

[18] Z. Zhao, B. Li, and Y. Jiang, "Effects of fracture surface roughness on macroscopic fluid flow and solute transport in fracture networks," *Rock Mechanics and Rock Engineering*, vol. 47, no. 6, pp. 2279–2286, 2014.

[19] R. Liu, B. Li, and Y. Jiang, "Critical hydraulic gradient for nonlinear flow through rock fracture networks: the roles of aperture, surface roughness, and number of intersections," *Advances in Water Resources*, vol. 88, pp. 53–65, 2016.

[20] J. Qian, M. Liang, Z. Chen, and H. Zhan, "Eddy correlations for water flow in a single fracture with abruptly changing aperture," *Hydrological Processes*, vol. 26, no. 22, pp. 3369–3377, 2012.

[21] A. A. Alrashed, O. A. Akbari, A. Heydari et al., "The numerical modeling of water/FMWCNT nanofluid flow and heat transfer in a backward-facing contracting channel," *Physica B: Condensed Matter*, vol. 537, pp. 176–183, 2018.

[22] W. Cherdron, F. Durst, and J. H. Whitelaw, "Asymmetric flows and instabilities in symmetric ducts with sudden expansions," *Journal of Fluid Mechanics*, vol. 84, no. 1, pp. 13–31, 1978.

[23] F. Durst, A. Melling, and J. H. Whitelaw, "Low Reynolds number flow over a plane symmetric sudden expansion," *Journal of Fluid Mechanics*, vol. 64, no. 1, pp. 111–128, 1974.

[24] F. Durst, J. C. F. Pereira, and C. Tropea, "The plane symmetric sudden-expansion flow at low Reynolds numbers," *Journal of Fluid Mechanics*, vol. 248, pp. 567–581, 1993.

[25] R. Fearn, T. Mullin, and K. Cliffe, "Nonlinear flow phenomena in a symmetric sudden expansion," *Journal of Fluid Mechanics*, vol. 211, pp. 595–608, 1990.

[26] S. A. Khan, A. Aabid, and M. A. A. Baig, "CFD analysis of CD nozzle and effect of nozzle pressure ratio on pressure and velocity for suddenly expanded flows," *International Journal of Mechanical and Production Engineering Research and Development*, vol. 8, no. 3, pp. 1147–1158, 2018.

[27] D. Badekas and D. Knight, "Eddy correlations for laminar axisymmetric sudden expansion flows," *Journal of Fluids Engineering*, vol. 114, no. 1, pp. 119–121, 1992.

[28] L. Ferrás, A. Afonso, M. Alves, J. Nóbrega, and F. Pinho, "Newtonian and viscoelastic fluid flows through an abrupt 1: 4 expansion with slip boundary conditions," *Physics of Fluids*, vol. 32, no. 4, article 043103, 2020.

[29] M. Rammane, S. Mesmoudi, A. Tri, B. Braikat, and N. Damil, "Bifurcation points and bifurcated branches in fluids mechanics by high-order mesh-free geometric progression algorithms," *International Journal for Numerical Methods in Fluids*, vol. 93, no. 3, pp. 834–852, 2021.

[30] M. Shapira, D. Degani, and D. Weihs, "Stability and existence of multiple solutions for viscous flow in suddenly enlarged channels," *Computers & Fluids*, vol. 18, no. 3, pp. 239–258, 1990.

[31] N. Alleborn, K. Nandakumar, H. Raszillier, and F. Durst, "Further contributions on the two-dimensional flow in a sudden expansion," *Journal of Fluid Mechanics*, vol. 330, pp. 169–188, 1997.

[32] J. Qian, L. Ma, H. Zhan, Q. Luo, X. Wang, and M. Wang, "The effect of expansion ratio on the critical Reynolds number in single fracture flow with sudden expansion," *Hydrological Processes*, vol. 30, no. 11, pp. 1718–1726, 2016.

[33] F. Battaglia, S. J. Tavener, A. K. Kulkarni, and C. L. Merkle, "Bifurcation of low Reynolds number flows in symmetric channels," *AIAA Journal*, vol. 35, no. 1, pp. 99–105, 1997.

[34] F. S. Milos, A. Acrivos, and J. Kim, "Steady flow past sudden expansions at large Reynolds number. II. Navier–Stokes solutions for the cascade expansion," *The Physics of Fluids*, vol. 30, no. 1, pp. 7–18, 1987.

[35] S. Makino, K. Iwamoto, and H. Kawamura, "Turbulent structures and statistics in turbulent channel flow with two- dimensional slits," *International Journal of Heat and Fluid Flow*, vol. 29, no. 3, pp. 602–611, 2008.

[36] Z. Chen, J. Qian, H. Zhan, Z. Zhou, J. Wang, and Y. Tan, "Effect of roughness on water flow through a synthetic single rough fracture," *Environmental Earth Sciences*, vol. 76, no. 4, 2017.

[37] J. Z. Qian, Z. Chen, H. B. Zhan, and H. C. Guan, "Experimental study of the effect of roughness and Reynolds number on fluid flow in rough-walled single fractures: a check of local cubic law," *Hydrological Processes*, vol. 25, no. 4, pp. 614–622, 2011.

[38] R. W. Zimmerman and I. W. Yeo, "Fluid flow in rock fractures: from the Navier-Stokes equations to the cubic law," in *Dynamics of Fluids in Fractured Rock*, B. Faybishenko, S. Benson, and P. Witherspoon, Eds., pp. 213–224, American Geophysical Union, Washington, 2000.

[39] S. R. Brown, "Fluid flow through rock joints: the effect of surface roughness," *Journal of Geophysical Research*, vol. 92, no. B2, pp. 1337–1347, 1987.

[40] G. M. Lomize, *Flow in Fractured Rocks*, Gosenergoizdat, Moscow, Russia, 1951.

[41] S. H. Lee, K. K. Lee, and I. W. Yeo, "Assessment of the validity of Stokes and Reynolds equations for fluid flow through a rough-walled fracture with flow imaging," *Geophysical Research Letters*, vol. 41, no. 13, pp. 4578–4585, 2014.

[42] P. Quinn, J. Cherry, and B. Parker, "Relationship between the critical Reynolds number and aperture for flow through single fractures: evidence from published laboratory studies," *Journal of Hydrology*, vol. 581, article 124384, 2020.

[43] P. A. Witherspoon, J. S. Y. Wang, K. Iwai, and J. E. Gale, "Validity of cubic law for fluid flow in a deformable rock fracture," *Water Resources Research*, vol. 16, no. 6, pp. 1016–1024, 1980.

[44] K. Xing, J. Qian, L. Ma, H. Ma, and W. Zhao, "Characterizing the scaling coefficient _ω_ between viscous and inertial permeability of fractures," *Journal of Hydrology*, vol. 593, article 125920, 2021.

[45] Y. Zhao, L. Zhang, W. Wang, J. Tang, H. Lin, and W. Wan, "Transient pulse test and morphological analysis of single rock fractures," *International Journal of Rock Mechanics and Mining Sciences*, vol. 91, pp. 139–154, 2017.

[46] F. Forchheimer, *The Prophylaxis and Treatment of Internal Diseases: Designed for the Use of Practitioners and of Advanced Students of Medicine*, D. Appleton & Company, 1906.

[47] S. E. Yochum, B. P. Bledsoe, E. Wohl, and G. C. L. David, "Spatial characterization of roughness elements in high-gradient channels of the Fraser Experimental Forest," *Water Resources Research*, vol. 50, no. 7, pp. 6015–6029, 2014.

[48] Y.-F. Chen, J.-Q. Zhou, S.-H. Hu, R. Hu, and C.-B. Zhou, "Evaluation of Forchheimer equation coefficients for non-Darcy flow in deformable rough-walled fractures," *Journal of Hydrology*, vol. 529, pp. 993–1006, 2015.

[49] C. Cherubini, C. Giasi, and N. Pastore, "Bench scale laboratory tests to analyze non-linear flow in fractured media," *Hydrology and Earth System Sciences*, vol. 16, no. 8, pp. 2511–2522, 2012.

[50] M. Javadi, M. Sharifzadeh, K. Shahriar, and Y. Mitani, "Critical Reynolds number for nonlinear flow through rough-walled fractures: the role of shear processes," *Water Resources Research*, vol. 50, no. 2, pp. 1789–1804, 2014.

[51] D. Ruth and H. Ma, "On the derivation of the Forchheimer equation by means of the averaging theorem," *Transport in Porous Media*, vol. 7, no. 3, pp. 255–264, 1992.

[52] Z. Zeng and R. Grigg, "A criterion for non-Darcy flow in porous media," *Transport in Porous Media*, vol. 63, no. 1, pp. 57–69, 2006.

[53] J.-Q. Zhou, S.-H. Hu, S. Fang, Y.-F. Chen, and C.-B. Zhou, "Nonlinear flow behavior at low Reynolds numbers through rough-walled fractures subjected to normal compressive loading," *International Journal of Rock Mechanics and Mining Sciences*, vol. 80, pp. 202–218, 2015.

[54] S. Briggs, B. W. Karney, and B. E. Sleep, "Numerical modeling of the effects of roughness on flow and eddy formation in fractures," *Journal of Rock Mechanics and Geotechnical Engineering*, vol. 9, no. 1, pp. 105–115, 2017.

[55] J. Schmittbuhl, A. Steyer, L. Jouniaux, and R. Toussaint, "Fracture morphology and viscous transport," *International Journal of Rock Mechanics and Mining Sciences*, vol. 45, no. 3, pp. 422–430, 2008.

[56] Z. Dou, Z. Chen, Z. Zhou, J. Wang, and Y. Huang, "Influence of eddies on conservative solute transport through a 2D single self- affine fracture," *International Journal of Heat and Mass Transfer*, vol. 121, pp. 597–606, 2018.

[57] H.-H. Liu, G. S. Bodvarsson, S. Lu, and F. J. Molz, "A corrected and generalized successive random additions algorithm for simulating fractional Levy motions," *Mathematical Geology*, vol. 36, no. 3, pp. 361–378, 2004.

[58] R. F. Voss, "Fractals in nature: from characterization to simulation," in *The Science of Fractal Images*, pp. 21–70, Springer, 1988.

[59] B. Launder and D. Spalding, *Mathematical Models of Turbulence*, Academic Press, London/New York, 1972.

[60] A. Restivo and J. H. Whitelaw, "Turbulence characteristics of the flow downstream of a symmetric, plane sudden expansion," *Journal of Fluids Engineering*, vol. 100, no. 3, pp. 308–310, 1978.

[61] E. Ghane, N. R. Fausey, and L. C. Brown, "Non-Darcy flow of water through woodchip media," *Journal of Hydrology*, vol. 519, pp. 3400–3409, 2014.

[62] P. Macini, E. Mesini, and R. Viola, "Laboratory measurements of non-Darcy flow coefficients in natural and artificial unconsolidated porous media," *Journal of Petroleum Science and Engineering*, vol. 77, no. 3-4, pp. 365–374, 2011.